AIAA JOURNAL
Vol. 47, No. 3, March 2009

# Eigensensitivity-Based Optimal Damper Location in Variable Geometry Trusses

A. Bilbao*
*IDOM Engineering, 48014 Vizcaya, Spain*
and
R. Avilés,† J. Aguirrebeitia,‡ and I. F. Bustos§
*Escuela Técnica Superior de Ingeniería, 48013 Vizcaya, Spain*

DOI: 10.2514/1.37353

**In this paper, two procedures are described to identify the optimal damping element locations in variable geometry trusses and to improve their behavior when dynamic loads are applied. In simple structures subjected to well-identified actions, obtaining an optimal location for damping elements can be relatively easy. However, as the geometry of the structures becomes more complex, the number of elements increases, and the frequency range of external actions is wider, finding the optimal location of dampers along the system becomes a difficult task. Furthermore, if the structure varies its geometry in successive positions, such as folding, unfolding, or any other movement, another level of complexity is added to the problem. The two procedures presented in this paper are based on calculating the effectiveness indices obtained from the derivatives of the eigenfrequencies of the dynamic eigenproblem with regard to parameters like stiffness or damping.**

## Nomenclature

$a_{ij}$ = modified effectiveness index of bar $j$ for vibration mode $i$
$\bar{a}_{ij}$ = effectiveness index of bar $j$ for vibration mode $i$
$b$ = index indicating the number of bars or possible locations of dampers
$b_{ij}$ = modified effectiveness index of bar $j$ for complex vibration mode $i$
$\bar{b}_{ij}$ = effectiveness index of bar $j$ for complex vibration mode $i$
$[C]$ = damping matrix
$c_j$ = damping coefficient of bar $j$
$p$ = index indicating the position or geometrical configuration of the variable geometry truss
$[K]$ = stiffness matrix
$k_j$ = stiffness coefficient of bar $j$
$[M]$ = mass matrix
$m$ = amount of vibration modes
$W_p$ = weight factor for position $p$
$w_i$ = weight factor for mode $i$
$\alpha_{ij}$ = normalized global effectiveness index of bar $j$ for vibration mode $i$
$\alpha_j$ = normalized global effectiveness index of bar $j$
$\lambda_i$ = eigenvalue $i$ of the nondamped dynamic eigenproblem.
$\{\varphi\}_i$ = eigenvector $i$ of the nondamped dynamic eigenproblem.
$\{\psi\}_i$ = eigenvector $i$ of the damped dynamic eigenproblem.
$\Omega_i$ = square root of eigenvalue $i$ of the damped dynamic eigenproblem.
$\omega_i$ = square root of eigenvalue $i$ of the nondamped dynamic eigenproblem.

Received 29 February 2008; revision received 28 October 2008; accepted for publication 20 November 2008. 

*Principal Design Engineer, Advanced Design & Analysis Group, Engineering & Consultancy, Bilbao; aba@idom.es.
†Professor, Department of Mechanical Engineering, Bilbao; rafael.aviles@ehu.es. Member AIAA.
‡Professor, Department of Mechanical Engineering, Bilbao; josu.aguirrebeitia@ehu.es.
§Professor, Department of Mechanical Engineering, Bilbao; impfedei@ehu.es.

## I. Introduction

IN RECENT decades, many researchers have been working to improve the dynamic behavior of structures, especially in the field of flexible space structures. Some of the results obtained for space structures have also been extrapolated to building structures subjected to seismic actions and slender structures subjected to forces caused by the wind. One way to control or reduce vibrations consists of optimally redesigning the structure geometry; in this regard, it is worth mentioning the works of Keane et al. [1–3] in which evolutionary optimization algorithms are employed to define structural geometries presenting better dynamic behavior in given frequency ranges. However, obtaining an optimal geometric design is not usually enough to ensure good dynamic behavior in structures. For example, the structures used in aerospace applications are, in general, very flexible and usually have small structural damping, whereas the geometric accuracy required is very high. Therefore, it is necessary to include damping elements (or even actuators), which can be passive, active, or semi-active. In the case of building structures subjected to dynamic actions, if slender elements are required, damping elements are also installed. Whether in the case of aerospace structures or building structures, an interesting problem is choosing the optimum locations of the damping elements. As possible damper location combinations are discrete, a combinatory optimization problem must be solved. In the following paragraphs, some alternatives for solving this problem are described briefly.

A first approach to obtaining the optimal combination of locating damper elements is established by the use of ad hoc iterative methods. Skelton and DeLorenzo [4] suggested starting by locating actuators in all possible locations and, afterward, eliminating the least effective one by one. Likewise, Haftka and Adelman [5] proposed another ad hoc iterative method to obtain quasioptimal solutions, in which only one actuator's location is changed in each iteration. These methods have a low computational cost but usually lead to nonoptimal designs.

A second approach to the problem consists of approximating the discrete optimization domain with a continuous domain. Once the optimization problem has been solved for the continuous domain, the damping elements are located in the discrete positions that best fit the continuous domain solution. Burdisso and Haftka [6] used this procedure to obtain the optimal locations of actuators in a space

structure holding an antenna, and Maghami and Joshi [7] also used it to locate actuators along a beam-shaped space truss. The loss of accuracy due to the use of a continuous domain instead of a discrete domain may be admissible. Nevertheless, the methodologies used in continuous optimization do not present significant computational advantages when compared with discrete optimization techniques.

A third approach is based on the use of effectiveness indices to quantify the fitness of the different locations of the actuators or dampers. In this way, Preumont et al. [8] suggested identifying the elements of a spatial truss structure that might be replaced by piezoelectric actuators used as active dampers and employing the modal elastic strain energy fraction of a given bar of the truss as the effectiveness index.

For effectiveness in a given modal range, the effectiveness index of each bar (each suitable location) is calculated as the weighted sum of the fractions of the elastic strain energy for each mode taken into account. This methodology assumes that the piezoelectric actuator replacing a bar would have approximately the same stiffness. This approach is also useful as a previous step to the more accurate combinatory optimization, to shortlist a subset of suitable location combinations and, therefore, to reduce the size of the problem. In this area, it is worthwhile mentioning the work done by Lammering et al. [9]; the optimization algorithm for the optimal PZT actuator placements uses the electric potentials to minimize the control effort.

A fourth approach is to solve the problem of combinatory optimization directly. It is the most accurate; however, it is also the most expensive. In this fourth approach, various alternative techniques can be used to solve the problem: integer linear programming methods, simulated annealing, and evolutionary methods such as genetic algorithms. For example, Ponslet et al. [10] and Padula and Sandridge [11] faced the optimal actuator location problem via integer linear programming. The aim of these works is to increase the damping in a given modal range. From a physical point of view, this method is analogous to the method of effectiveness indeces established by Preumont et al. [8]; however, there is a difference in the mathematical solving procedure. This method is very intuitive for an engineer, though it sometimes presents low numerical effectiveness when the modal range to be taken into account is high or when the effect of each actuator in the total damping is high and considering the effects of many actuators as an additive is impossible.

The methods established based on simulated annealing or genetic algorithms are the most accurate but are also computationally expensive. The method of simulated annealing (introduced by Metropolis et al. [12]) may be considered an improvement over the aforementioned iterative methods [4,5]. Chen et al. [13,14] applied the method of simulated annealing to the search for optimal locations of passive and active actuators. They proposed a procedure in which a location occupied by an actuator is both selected randomly and randomly changed to a different location unoccupied by any other actuator. The objective function arranged for the optimization process is the total summation of the energy dissipated by the passive and active actuators for a finite time interval, this interval being approximately 3 times the period of the first eigenfrequency.

Lastly, the evolutionary methods and, especially, genetic algorithms (pioneered by Holland [15]) are currently the more extended heuristic methods used to solve the problem of optimally locating actuators in structures. The genetic algorithm method is more recent than simulated annealing and is more effective in the field of solution improvement. As such, some of the first works about the use of genetic algorithms in the field of determining damper and actuator optimal location in space structures are outlined. Rao et al. [16] used a genetic algorithm to search for the optimal locations of three active actuators along a ten-bar space structure taken as an example. To do this, they used a binary codification in such a way that a *zero* value implies a location without an actuator and a *one* value implies a location with an actuator, that is, each chromosome is a binary chain with three *one* values and seven *zero* values. Onoda and Hanawa [17] described a simulated annealing methodology, including some features typically belonging to a genetic algorithm, and applied it to the selection of actuator optimal locations in space structures with more than 200 bars. It is also interesting to point out the work of Dhingra and Lee [18], in which a genetic algorithm is used, hybridized with steepest descent optimization techniques. The genetic algorithm generates some populations for a given progeny number and, in a final step, the steepest descent optimization techniques are applied, taking as a starting point the solution given by the last genetic algorithm iteration. The fitness function arranged as the optimal location criteria is the amount of energy dissipated by the actuator during a predefined time interval.

In 1995, Furuya and Haftka [19] proposed searching for optimal locations via some kind of effectiveness indeces, as Preumont et al. [8] did, but using them as a fitness function for the genetic algorithm. The advantage of employing effectiveness indices as fitness functions instead of calculating the dissipated energy integral by actuators is the speed with which they are computed. This is especially advantageous in the case of genetic algorithms due to the great number of iterations required. As a disadvantage, the effectiveness indices present the limitation of being less accurate than the calculation of the integral of the dissipated energy.

Recently, the use of genetic algorithms to search for optimal damper locations has also been extended to building structures to improve their behavior against seismic or wind loads, as mentioned in [20–24]. When dealing with space structures, the search for optimal actuator locations is still a research area in and of itself. A large amount of work in this field is centered on the use of genetic algorithms, developing new fitness functions for specific objectives defined in each case, and/or advances in the efficiency of genetic algorithms themselves, as indicated, for example, in [25].

In the following sections, two new methods are presented to search for the optimal damper locations following a system analogous to the one used by Preumont et al. [8] but with an appreciably different theoretical approach. Specifically, the development presented in this work is established on a technique based on the calculation of real eigenvalue derivatives, as in Fox and Kapoor [26], and complex eigenvalue derivatives, as in Adhikari [27], known as an "eigensensitivity analysis." An effectiveness index approach has been chosen due to computational saving advantages; therefore, it is considered the most appropriate for application to variable geometry trusses (VGTs), for which an optimal location is to be obtained not only for a unique geometrical configuration but also for a series of different geometries given by a set of successive positions. In the same way, the authors propose hybridizing this methodology with genetic algorithms in the future. In Fig. 1, a prototype of a variable geometry truss developed by the authors is shown.

Application examples are presented and discussed after the theoretical explanation of each of the two approaches. In addition, these examples are used to go more deeply into some important features of the method.

## II. Optimal Damper Positioning Using Real Eigensensitivity

An intuitive way to detect the optimal location of a damper (situated parallel to a bar of the structure) to be effective is to determine how a change in the stiffness of that bar affects the natural frequencies of the structure. In fact, if a given bar is accompanied by a damper, the result is in some way equivalent to introducing an additional force between the nodes of that bar. If the stiffness of the bar is increased, the result is also equivalent to introducing an additional force between the nodes of the bar. In the case of increasing the stiffness, the force is proportional to the difference of the nodal displacements in the direction of the bar, whereas by adding a damper the force is proportional to the difference of the nodal velocities. In other words, the highest changes in natural frequencies are obtained by increasing the stiffness of the bars with high strain energy, which would also dissipate high damping energy.

According to the preceding paragraph, one can postulate that the effectiveness of locating a damper in a given position can be measured as the influence that the increase in the stiffness of a bar, located in parallel with the damper, would have on the natural frequencies. This method is also valid when a damper is wanted

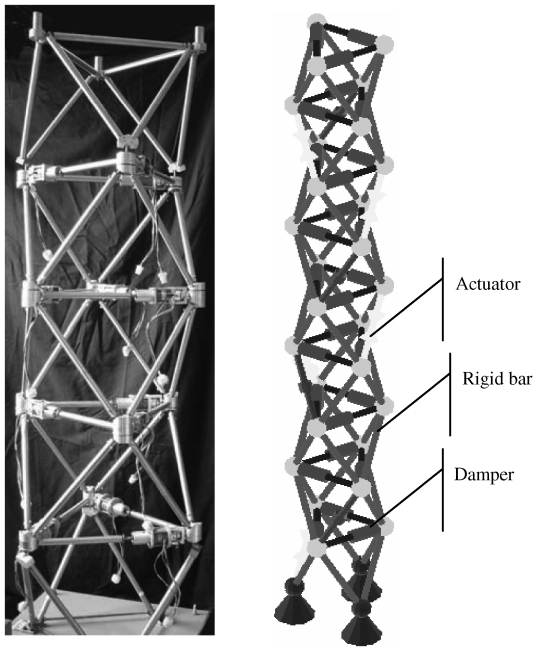


a) Prototype of VGT. MBAD work team b) General diagram of a VGT

**Fig. 1 Variable geometry trusses (where MBAD refers to multibody analysis and design).**

between nodes not joined with a bar; in this case, the initial stiffness would be zero.

To determine the sensitivity of a natural frequency to the variation in bar stiffness, the derivative of that natural frequency must be calculated in relation to its stiffness coefficient. For each natural vibration mode of interest, the corresponding natural frequency derivatives must be calculated in relation to the stiffness coefficients of each bar in the structure. Optimal locations to place a damper will be given by those for which these derivatives are the highest. In this way, some effectiveness indices are defined for each location and selected vibration mode. Let $\omega_i$ be the natural frequency of mode $i$, within the modal range of vibrations requiring attenuation, and $k_j$ the stiffness coefficient of bar $j$ of the structure; the effectiveness index $\bar{a}_{ij}$ for mode $i$ in the location given by $j$ would be defined as

$$\bar{a}_{ij} = \frac{\partial \omega_i}{\partial k_j} \tag{1}$$

To simplify calculation of the expression of the derivatives, we propose the squared natural frequency derivative be taken instead of that given by Eq. (1), that is, the eigenvalue derivative $\lambda_i$ of the nondamped dynamic eigenproblem with respect to bar stiffness $j$.

$$a_{ij} = \frac{\partial \omega_i^2}{\partial k_j} = \frac{\partial \lambda_i}{\partial k_j} \tag{2}$$

To determine the derivative of Eq. (2), the expression developed by Fox and Kapoor [26] is applied, based on previously obtaining the characteristic equation derivative of eigenvalues and eigenvectors:

$$a_{ij} = \frac{\partial \lambda_i}{\partial k_j} = \{\varphi\}_i^T \left[ \frac{\partial [K]}{\partial k_j} - \lambda_i \frac{\partial [M]}{\partial k_j} \right] \{\varphi\}_i \tag{3}$$

where $\{\varphi\}_i$ is the natural mode $i$, and $[K]$ and $[M]$ are the stiffness and mass matrices of the structure, respectively. As the mass matrix does not depend on the stiffness of the bars,

$$\frac{\partial [M]}{\partial k_j} = 0 \tag{4}$$

and, therefore,

$$a_{ij} = \frac{\partial \lambda_i}{\partial k_j} = \{\varphi\}_i^T \left[ \frac{\partial [K]}{\partial k_j} \right] \{\varphi\}_i \tag{5}$$

The stiffness matrix of a structure can be expressed as the following summation:

$$[K] = \sum_{e=1}^{b} k_e [\bar{g}_e] \tag{6}$$

where $b$ is the total amount of bars in the structure and $[\bar{g}_e]$ is the element geometric matrix for bar $e$, expanded to the total amount of degrees of freedom in the system, as described in the works of Avilés et al. [28,29]. Therefore, the stiffness matrix derivative can be formulated as follows:

$$\frac{\partial [K]}{\partial k_j} = \frac{\partial}{\partial k_j} \left( \sum_{e=1}^{b} k_e [\bar{g}_e] \right) = \sum_{e=1}^{b} \frac{\partial k_e}{\partial k_j} [\bar{g}_e] + k_e \frac{\partial [\bar{g}_j]}{\partial k_j} \tag{7}$$

The geometric matrix depends on geometric parameters only (as deduced from its name); if the VGT is formed only by bars articulated via spherical pairs, these parameters are only the angles that fix the bar location. Therefore, the derivative takes the following value:

$$\frac{\partial [K]}{\partial k_j} = \sum_{e=1}^{b} \delta_{ej} [\bar{g}_e] + k_e \cdot 0 \tag{8}$$

where $\delta_{ej}$ is null if $e \neq j$ and unity if $e = j$, that is,

$$\frac{\partial [K]}{\partial k_j} = [\bar{g}_j] \tag{9}$$

Therefore, the effectiveness indices can be calculated from the following expression:

$$a_{ij} = \frac{\partial \lambda_i}{\partial k_j} = \{\varphi\}_i^T [\bar{g}_j] \{\varphi\}_i \tag{10}$$

## III. Examples of Damper Positioning Using Real Eigensensitivity

The examples developed in this paper correspond to the six-module variable geometry truss shown in Fig. 2. The bars of the structure, whose limit nodes are detailed in Table 1, are joined via spherical joints. The lengths of the bars range from 0.6 to 1.5 m, their section area is $1.2 \times 10^{-4}$ m$^2$, and the material is steel, with a density of $7.8 \times 10^3$ kg/m$^3$ and a Young modulus of $2.1 \times 10^{11}$ Pa. The displacements of the three nodes at the base are constrained. It has been assumed that the mass of all the bars is the same regardless of length to avoid problems with active bars (high displacement actuators). The assumed mass value is 0.936 kg (corresponding to a 1.0 m length). The stiffness of the bars has also been taken regardless of bar length and its value is $2.52 \times 10^7$ N/m. In Fig. 3, the shape of the lowest four modes is shown for the VGT in Fig. 2.

This structure with 57 bars is complex enough to justify an alternative method to that given by a full search method. If one could know how many different combinations would be necessary to evaluate the location of four dampers (considering them parallel to existing bars), $\binom{57}{4} = 39.395.010$ evaluations would have to be made.

### A. Example 1

Effectiveness indices are calculated for each bar in the structure according to Eq. (10) and for the lowest four natural modes. These indices are normalized to be uniformly represented via scaling with respect to the maximum per mode:

$$\alpha_{ij} = a_{ij} / A_i \tag{11}$$

where

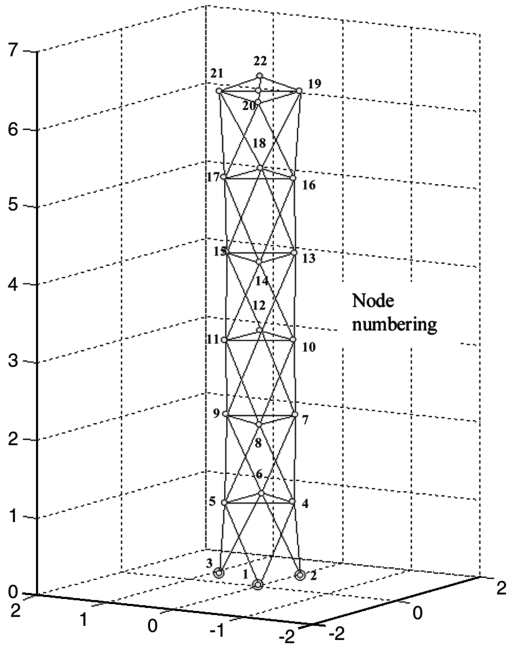


**Fig. 2 Six-module VGT used in the examples.**

$$A_i = \max\{a_{i1}, a_{i2}, \ldots, a_{ij}, \ldots, a_{ib}\} \tag{12}$$

The results of the effectiveness indices appear in Fig. 4. In this figure, the locations with the four highest effectiveness indices appear drawn with thick stroke; these locations would be the best for damping elements to improve the dynamic behavior of the structure against vibrations exciting the lowest four vibration modes.

When comparing the locations with greater effectiveness indices with the shape of the vibration modes, it is especially significant that for the first mode (geometrically equivalent to the first flexural mode in a cantilever beam) the positions of highest effectiveness are all located at the structure base, whereas for the fourth mode (geometrically equivalent to the second flexural mode in a cantilever beam) some high indexed locations appear in the middle of the structure, in a zone in which the corresponding mode has an inflection point. Analogous reasoning has also been considered in a recent paper by Gao [30].

To take into account many vibration modes, first the effectiveness indices corresponding to each mode must be normalized using the expressions given in Eqs. (11) and (12) and, afterward, a global effectiveness index must be calculated for each location as the summation of the normalized effectiveness indices of each vibration mode. From these normalized effectiveness indices, a global index, $\alpha_j$, is calculated for each location to cover the modal range required. For example, if damper placing is considered to attenuate a vibration that excites the vibration modes ranging from 1 to $m$, the expression to be used is

$$\alpha_j = \sum_{i=1}^{m} \frac{a_{ij}}{A_i} = \sum_{i=1}^{m} \alpha_{ij} \tag{13}$$

### B. Example 2

For the same structure used in the previous example, Fig. 5 shows the results of the global effectiveness indices calculated for the lowest four natural modes according to Eq. (13). In the same figure, the four optimal locations to control vibrations exciting the lowest four vibration modes are shown with a thick stroke.

In addition, if there are some vibration modes for which attenuation is more interesting than for others, a weighting operation can be performed. For example, Furuya and Haftka [19] analyzed weighting strategies in which more importance is given to the first or lowest mode as compared with the highest. However, weighting factors can be established dealing with other priorities, for example, vibrations provoking displacements in the structure when high positioning precision is required or positions near an obstacle to avoid collisions. Let $w_i$ be the weighting factor corresponding to vibration mode $i$; the global weighted effectiveness indices can be calculated as the summation given by Eq. (14):

$$\alpha_j = \sum_{i=1}^{m} w_i \frac{a_{ij}}{A_i} = \sum_{i=1}^{m} w_i \alpha_{ij} \tag{14}$$

### C. Example 3

In this example, the same global effectiveness index calculation is performed as in example 2, but the contribution of each mode is weighted with different values. In this case, the weighting factors have been chosen as 1, 1, 3, and 2 for modes 1, 2, 3, and 4, respectively, that is, more importance has been given to mode 3 and then to mode 4, and less importance to modes 1 and 2. Figure 6 shows the results. One can observe that the graph of effectiveness indices has been modified with respect to the graph shown in Fig. 5.

The weighted global effectiveness indices calculated with Eq. (14) are valid for one position in the structure, that is, for only one geometrical configuration. To apply this methodology to variable geometry trusses, the expressions for the effectiveness indices must be generalized; therefore, successive positions reached by the VGT must be considered. Therefore, in general, the weighting must be

**Table 1 Bar list for VGT in Fig. 2**

| Bar ID | Node 1 | Node 2 | Bar ID | Node 1 | Node 2 | Bar ID | Node 1 | Node 2 |
|---|---|---|---|---|---|---|---|---|
| 1 | 2 | 4 | 20 | 7 | 12 | 39 | 15 | 17 |
| 2 | 2 | 6 | 21 | 9 | 11 | 40 | 15 | 18 |
| 3 | 1 | 4 | 22 | 9 | 12 | 41 | 14 | 16 |
| 4 | 1 | 5 | 23 | 8 | 10 | 42 | 14 | 17 |
| 5 | 3 | 6 | 24 | 8 | 11 | 43 | 16 | 19 |
| 6 | 3 | 5 | 25 | 10 | 13 | 44 | 18 | 19 |
| 7 | 4 | 8 | 26 | 12 | 13 | 45 | 16 | 20 |
| 8 | 5 | 8 | 27 | 10 | 14 | 46 | 17 | 20 |
| 9 | 6 | 9 | 28 | 11 | 14 | 47 | 17 | 21 |
| 10 | 5 | 9 | 29 | 11 | 15 | 48 | 18 | 21 |
| 11 | 6 | 7 | 30 | 12 | 15 | 49 | 16 | 17 |
| 12 | 4 | 7 | 31 | 10 | 11 | 50 | 17 | 18 |
| 13 | 4 | 6 | 32 | 11 | 12 | 51 | 18 | 16 |
| 14 | 6 | 5 | 33 | 12 | 10 | 52 | 19 | 20 |
| 15 | 5 | 4 | 34 | 13 | 14 | 53 | 20 | 21 |
| 16 | 7 | 8 | 35 | 14 | 15 | 54 | 21 | 19 |
| 17 | 8 | 9 | 36 | 15 | 13 | 55 | 19 | 22 |
| 18 | 9 | 7 | 37 | 13 | 16 | 56 | 22 | 21 |
| 19 | 7 | 10 | 38 | 13 | 18 | 57 | 22 | 20 |

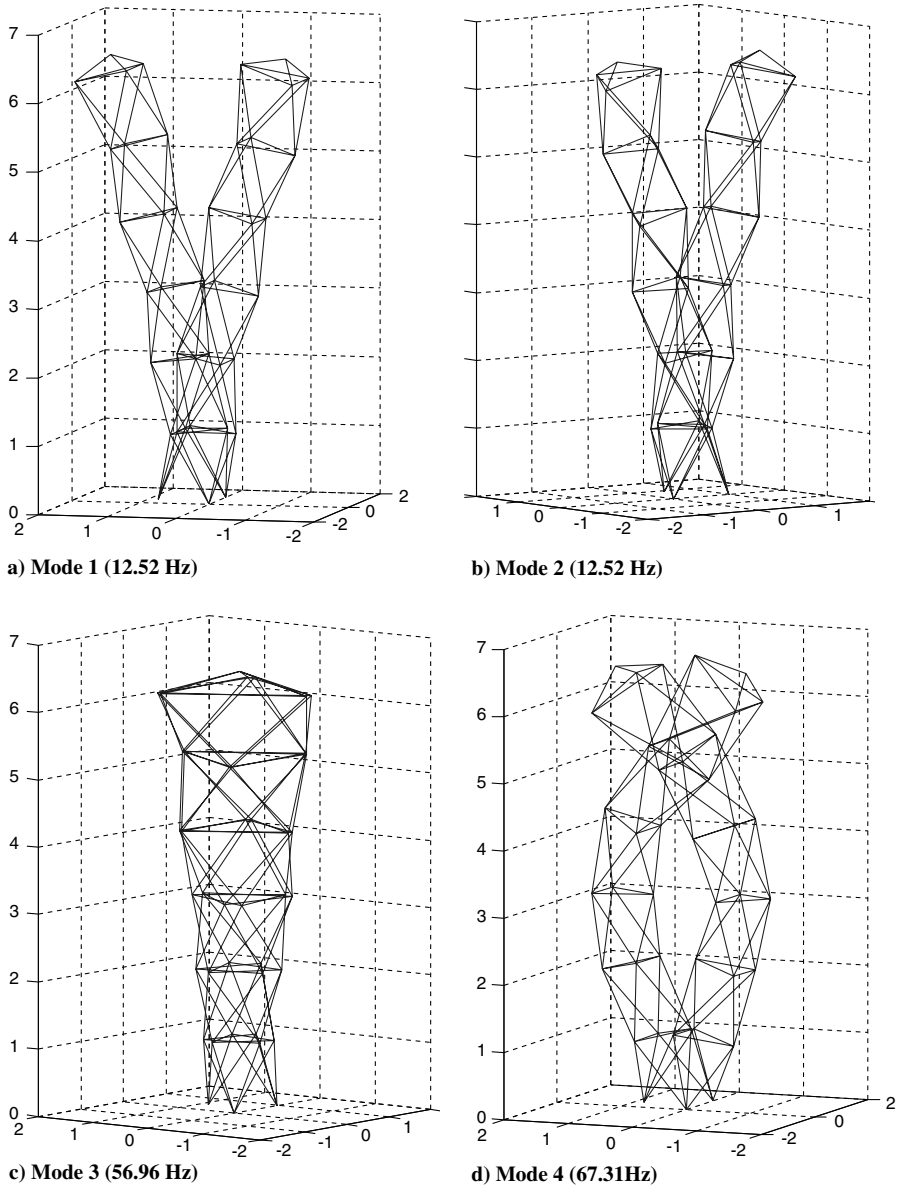

a) Mode 1 (12.52 Hz) b) Mode 2 (12.52 Hz)

c) Mode 3 (56.96 Hz) d) Mode 4 (67.31Hz)

**Fig. 3 Vibration modes of the six-bar VGT.**

double; apart from the modal weighting proposed in Eq. (14), a second weighting needs to be considered, dealing with the successive structure positions. To do so, first the VGT path must be discretized in $n$ successive positions to be representative of the entire movement. For each position $p$ of the structure, the effectiveness index for each location $j$ is calculated as

$$\alpha_{j,p} = \sum_{i=1}^{m} w_{i,p} \frac{a_{ij,p}}{A_{i,p}} = \sum_{i=1}^{m} w_{i,p} \alpha_{ij,p} \tag{15}$$

Therefore, the effectiveness index of location $j$ for the modes ranging from 1 to $m$ and for all the successive positions ranging from 1 to $n$ must be calculated with the double summation of Eq. (16):

$$\alpha_{j} = \sum_{p=1}^{n} \sum_{i=1}^{m} w_{i,p} \frac{a_{ij,p}}{A_{i,p}} = \sum_{p=1}^{n} \sum_{i=1}^{m} w_{i,p} \alpha_{ij,p} \tag{16}$$

In the same way, weighting factors can be included to take into account the different relative importance among positions; it may be interesting to give more weight to those positions at which greater accuracy is required. The following expression can be used when position weighting factors are taken into account:

$$\alpha_{j} = \sum_{p=1}^{n} W_{p} \sum_{i=1}^{m} w_{i,p} \frac{a_{ij,p}}{A_{i,p}} = \sum_{p=1}^{n} W_{p} \sum_{i=1}^{m} w_{i,p} \alpha_{ij,p} \tag{17}$$

where $W_p$ is the weighting factor for position $p$. It must be mentioned that the modal weighting factor for each mode $i$ can be different for different positions, that is, in general, $w_{i,p1} \neq w_{i,p2}$. In this way, it is possible to attenuate some modes in a position range and some others in another position range.

Finally, it must be also mentioned that the expression given by Eq. (17), established to determine the global weighted effectiveness indices by taking into account different modal and position ranges, is not entirely correct. The position weighting factors $W_p$ might have an equivalent contribution when building the effectiveness index, before application of the position weighting factor. To achieve that equivalence, a second normalization should be performed before $W_p$ is applied, which can be established by defining the normalization factor $B_p$ as in Eq. (18).

$$B_{p} = \max_{j=1,b} \left\{ \sum_{i=1}^{m} w_{i,p} \frac{a_{ij,p}}{A_{i,p}} \right\} = \max_{j=1,b} \left\{ \sum_{i=1}^{m} w_{i,p} \alpha_{ij,p} \right\} \tag{18}$$

With this factor, the effectiveness indices can be redefined as in Eq. (19).

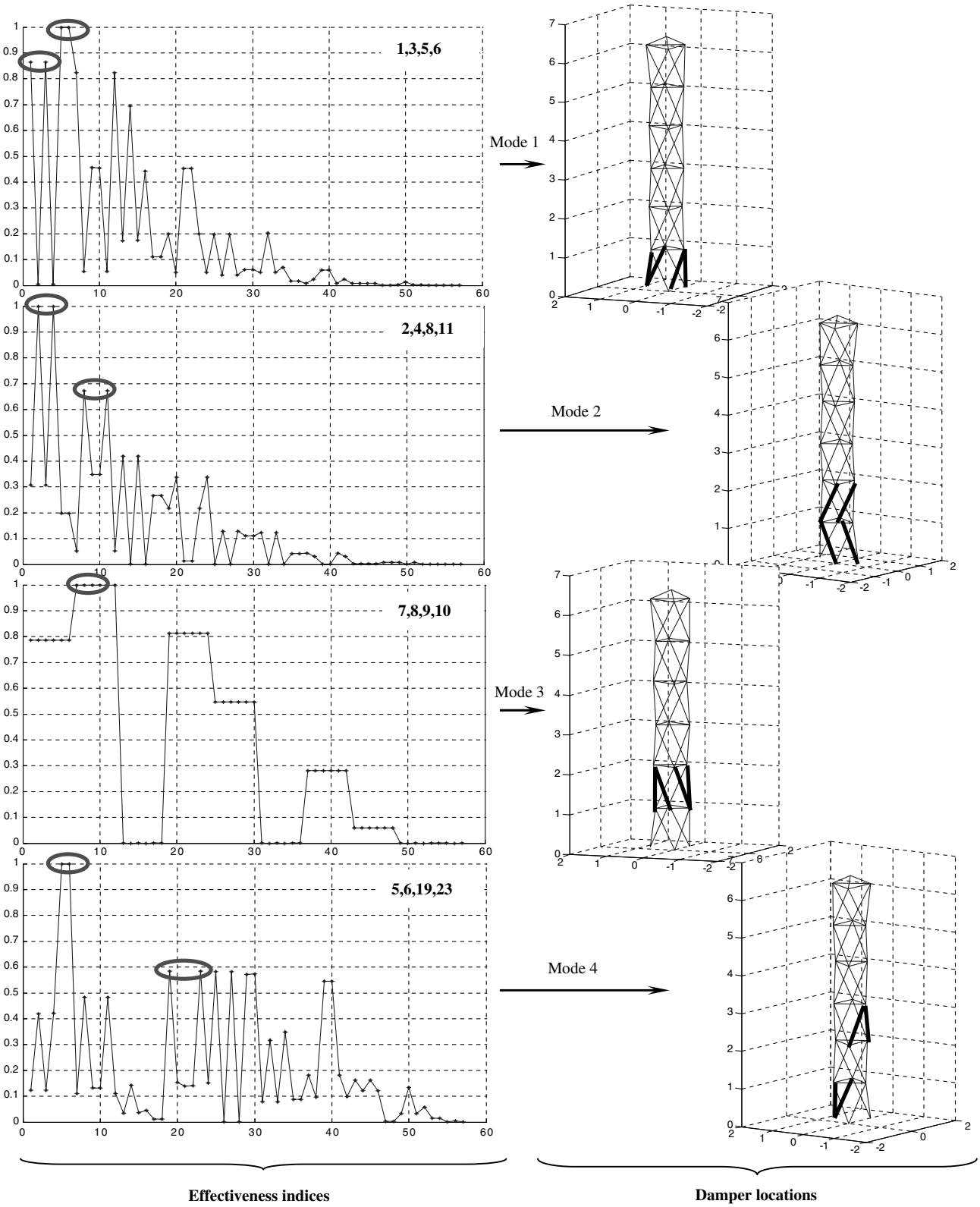


**Fig. 4 Location of four dampers to attenuate the lowest four modes.**

$$\alpha_j = \sum_{p=1}^{n} W_p \frac{\sum_{i=1}^{m} w_{i,p}\alpha_{ij,p}}{B_p} \tag{19}$$

When generalization of successive geometric positions is required, the main difficulty derives from the calculations of $a_{ij,p}$:

$$a_{ij,p} = \left.\frac{\partial \lambda_i}{\partial k_j}\right|_p = \{\varphi\}_{i,p}^T [\bar{g}_j]_p \{\varphi\}_{i,p} \tag{20}$$

As can be observed in Eq. (20), recalculation of the eigenvectors and geometric matrix is required for each new position. The calculation of the geometric matrix for each position is straightforward, and only the values of the angles defining the direction of the bars must be updated in the corresponding expressions. However, the eigenproblem must be solved again for each new position to determine new eigenvalues and eigenvectors, which may be computationally expensive. As an alternative strategy to minimize computational cost, eigenvector linear estimation is

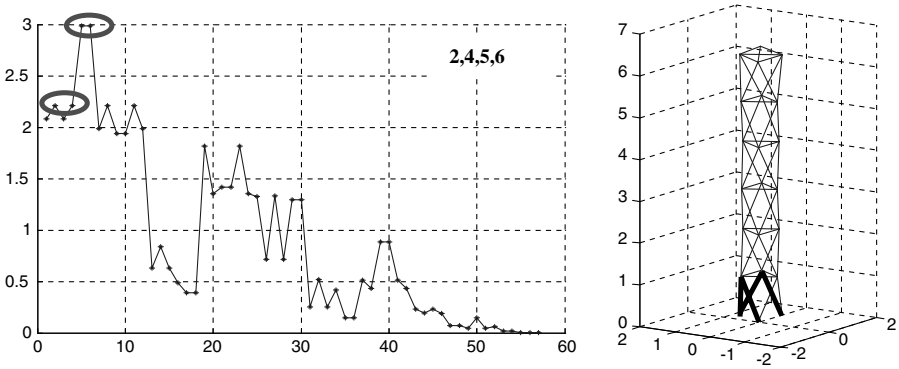


**a) Global effectiveness indices** **b) Damper locations**

**Fig. 5 Location of four dampers to attenuate the lowest four vibration modes.**

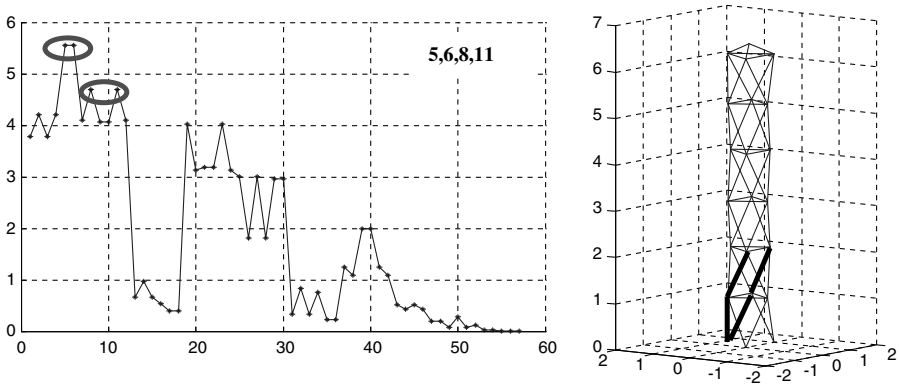


**a) Global effectiveness indices** **b) Damper location**

**Fig. 6 Location of four dampers to attenuate the four lowest modes with weighting factors (1, 1, 3, 2).**

proposed for each new position $\{x\} + \Delta\{x\}$, taking the previous position $\{x\}$ as a starting point:

$$\{\bar{\varphi}\}_i|_{\{x\}+\Delta\{x\}} = \{\varphi\}_i|_{\{x\}} + \left[\frac{\partial\{\varphi\}_i}{\partial\{x\}}\right]^T\Bigg|_{\{x\}} \Delta\{x\} \tag{21}$$

If great geometric variations occur along the structure movement, the eigenproblem may be solved periodically to ensure the fidelity of the estimations. In any case, a great amount of computation time might be saved by not having to solve an eigenproblem per position. In Fig. 7, a flowchart of the complete, real eigensensitivity-based methodology to calculate effectiveness indices when successive positions are taken into account for the VGT is shown.

### D. Example 4

In Fig. 9, the damper optimal locations are shown to control the lowest four vibration modes (without any weighting factor) for the entire deployment operation of the same VGT used in previous examples. In Fig. 8, the deployment operation can be observed in six frames.

## IV. Optimal Damper Positioning Using Complex Eigensensitivity

The methodology developed in the previous section presupposes that the effect of the damping elements can be estimated from the nondamped original VGT; therefore, the real eigensensitivity is assumed to have been applied, that is, not taking into account the effect of dampers included in the structure modal response. The error of this approximation is smaller as the number of dampers and damping rate decrease in the VGT. For example, Padula and Sandridge [11] and Metropolis et al. [12] rejected the influence of damping in modal analysis, restricting the number of dampers to eight. The best way to measure the effectiveness of the dampers is to calculate the energy they dissipate via numerical time integration; however, as shown in the works of Chen et al. [14] and Rao et al. [16], these methods are computationally very expensive. In a VGT, for which many geometrical configurations must be taken into account, finding approximate solutions is very important to save computational time.

In this sense, the methodology developed herein can be generalized to work with complex modes, increasing the accuracy of the effectiveness indices; the development shown in this section is the result of that generalization. The computational cost is slightly increased yet remains below the cost of direct numeric integration required by the calculation of the dissipated energy of the dampers. At the same time, the method developed here allows a sequential optimal damper location search, that is, adding damping elements one by one or group by group if required, and supposes an easy practical alternative to the problem of combinatory optimization.

In the previous section, the question was "Where is the best location to put a damper?" And the answer was the location where the natural frequencies of the nondamped VGT have maximum sensitivity to the stiffness of the bar located there. The generalization now considered modifies the answer: the location where the complex eigenvalues of a damped VGT have maximum sensitivity to the damping coefficient of a possible damper located there.

As in Sec. II, to determine the sensitivity of a damped frequency in a bar, its derivative is calculated with respect to the damping coefficient of a damper located in parallel. And for each interesting vibration mode, the derivative of the corresponding damped frequency must be calculated with respect to the damping coefficient in each possible location in the structure. The optimal locations of the dampers are the most eigensensitive locations.

The equation governing the vibrations in a finite element method model of a damped mechanical system is given by Eq. (22):

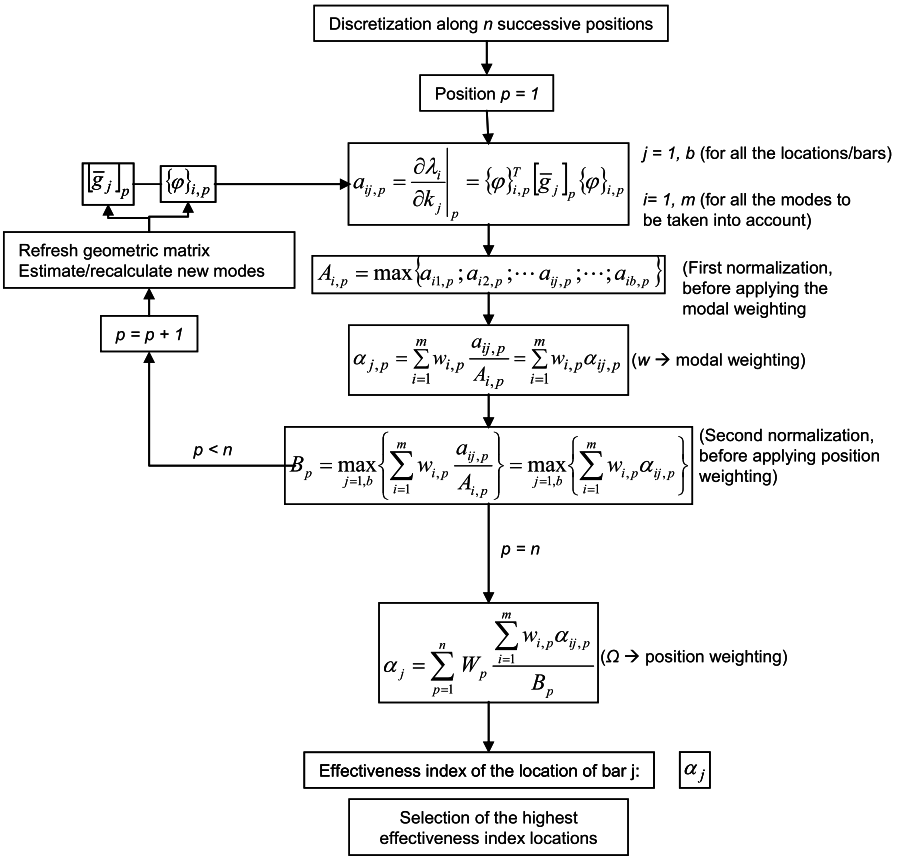


**Fig. 7 Flowchart of optimal damper positioning based on real eigensensitivity.**

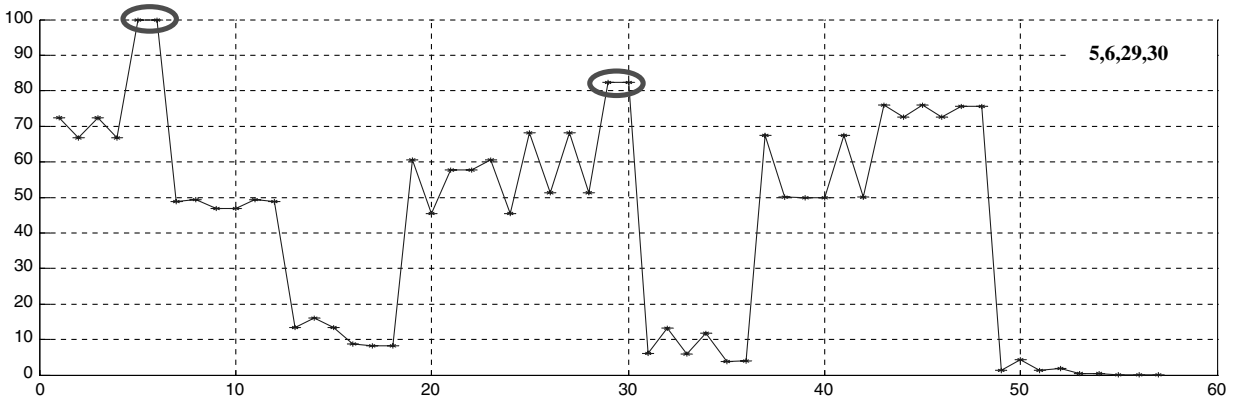


**a) Global effectiveness indices**

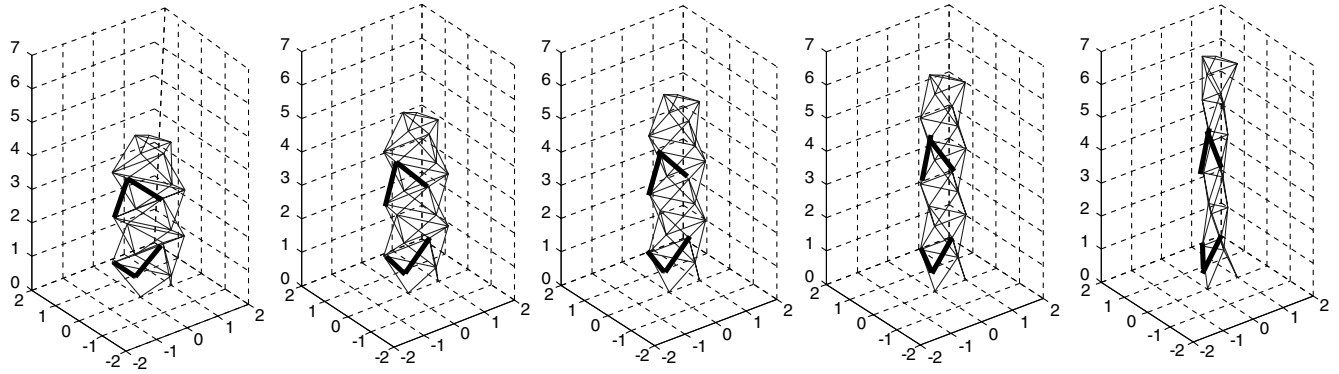

**b) Optimal damper locations**

**Fig. 8 Damper location to attenuate the lowest four vibration modes (successive positions).**

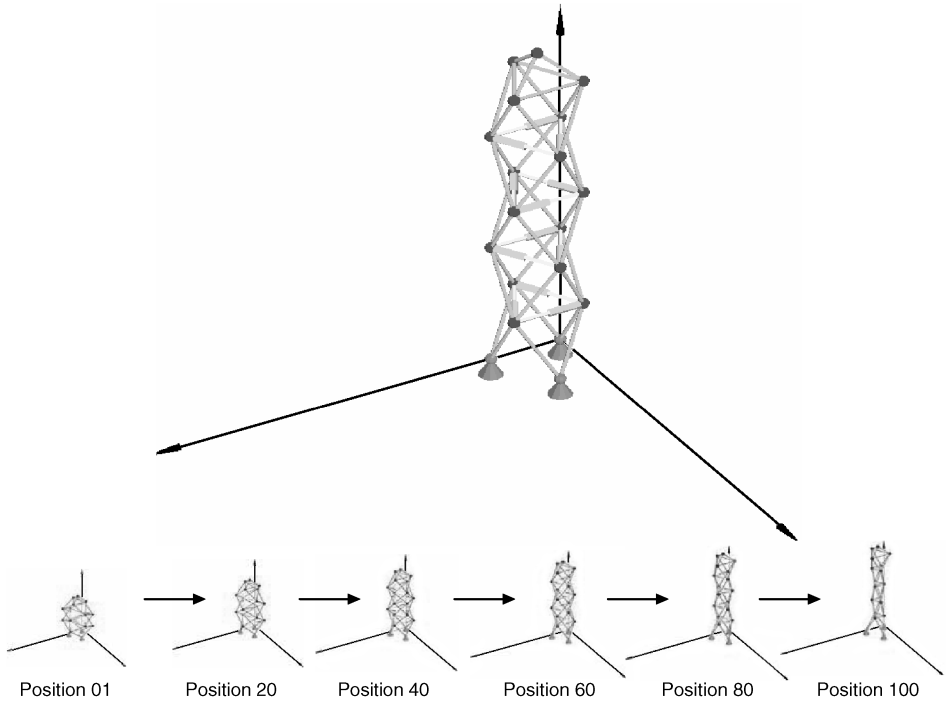


**Fig. 9 Deployment operation of a VGT.**

$$[M]\{\ddot{\delta}(t)\} + [C]\{\dot{\delta}(t)\} + [K]\{\delta(t)\} = \{0\} \tag{22}$$

where $[M]$ is the mass matrix, $[C]$ is the damping matrix, and $[K]$ is the stiffness matrix. $\{\delta(t)\}$, $\{\dot{\delta}(t)\}$, and $\{\ddot{\delta}(t)\}$ are the nodal displacement, velocity, and acceleration vectors, respectively. Harmonic solutions to the previous equations exist as

$$\left.\begin{array}{l} \{\delta(t)\} = \{\psi\}e^{st} \\ s = i\Omega; i = \sqrt{-1} \end{array}\right\} \tag{23}$$

where $\{\psi\}$ is a complex eigenvector and $s = i\Omega$ is a complex eigenvalue. Substituting Eq. (23) in Eq. (22), we obtain

$$s^2[M]\{\psi\} + s[C]\{\psi\} + [K]\{\psi\} = \{0\} \tag{24}$$

that is,

$$(s^2[M] + s[C] + [K])\{\psi\} = \{0\} \tag{25}$$

When the damping matrix is null, these complex eigenvalues match real natural frequencies:

$$[C] = [0] \Rightarrow \Omega = \omega \tag{26}$$

The effectiveness indices are to be calculated from the derivatives of the damped frequencies with respect to the damping coefficient $c_j$ of each possible location $j$ (parallel to the bars of the structure). Adhikari [27] demonstrated that the expression of this derivative is

$$\frac{\partial \Omega_i}{\partial c_j} = \Omega_i \frac{\{\psi\}_i^T (\frac{\partial [K]}{\partial c_j} - \Omega_i^2 \frac{\partial [M]}{\partial c_j} + i\Omega_i \frac{\partial [C]}{\partial c_j})\{\psi\}_i}{\{\psi\}_i^T (\Omega_i^2[M] + [K])\{\psi\}_i} \tag{27}$$

The previous expression itself defines the new proposed effectiveness index of location $j$ for vibration complex mode $i$:

$$\bar{b}_{ij} = \frac{\partial \Omega_i}{\partial c_j} \tag{28}$$

In this case, the effectiveness of arranging a damper is measured parallel to the bar $j$ to attenuate the vibration complex mode $i$. Equation (27) can be developed by taking into account that neither the mass matrix nor the stiffness matrix are damping dependent:

$$\left.\begin{array}{l} \frac{\partial [K]}{\partial c_j} = 0 \\ \frac{\partial [M]}{\partial c_j} = 0 \end{array}\right\} \tag{29}$$

Therefore, Eq. (27) can be simplified as follows:

$$\bar{b}_{ij} = \frac{\partial \Omega_i}{\partial c_j} = \Omega_i \frac{\{\psi\}_i^T (i\Omega_i \frac{\partial [C]}{\partial c_j})\{\psi\}_i}{\{\psi\}_i^T (\Omega_i^2[M] + [K])\{\psi\}_i} \tag{30}$$

To calculate the previous expression, first the damping matrix derivative with respect to the damping coefficient $c_j$ is required. As Bilbao et al. [31] demonstrated, if discrete dampers are arranged parallel to the bars of a VGT, the damping matrix can be expressed as a function of the expanded element geometric matrices:

$$[C] = \sum_e^b c_e[\bar{g}_e] \tag{31}$$

where $b$ is the total amount of possible locations. Therefore,

$$\frac{\partial [C]}{\partial c_j} = \sum_{e=1}^{b} \delta_{ej}[\bar{g}_e] + c_e \cdot 0 \tag{32}$$

where $\delta_{ej}$ is null if $e \neq j$ and unity if $e = j$, that is,

$$\frac{\partial [C]}{\partial c_j} = [\bar{g}_j] \tag{33}$$

One can observe that the derivative in Eq. (33) matches the derivative in Eq. (9). Therefore, the effectiveness indices $\bar{b}_{ij}$ can be calculated as

$$\bar{b}_{ij} = \Omega_i \frac{\{\psi\}_i^T (i\Omega_i[\bar{g}_j])\{\psi\}_i}{\{\psi\}_i^T (\Omega_i^2[M] + [K])\{\psi\}_i} \tag{34}$$

This leads to

$$\bar{b}_{ij} = i\Omega_i^2 \frac{\{\psi\}_i^T [\bar{g}_j]\{\psi\}_i}{\{\psi\}_i^T (\Omega_i^2[M] + [K])\{\psi\}_i} \tag{35}$$

When applying these effectiveness indices to the search for the optimal damper location, first the nondamped situation must be chosen as the starting point. For this initial situation, the frequencies and $e$ modes will be real:

$$\left.\begin{array}{c}\{\psi\}_{i,o}=\{\varphi\}_i\\ \Omega_{i,o}=\omega_i\end{array}\right\} \tag{36}$$

Therefore,

$$\bar{b}_{ij,o}=i\omega_i^2\frac{\{\varphi\}_i^T[\bar{g}_j]\{\varphi\}_i}{\{\varphi\}_i^T(\omega_i^2[M]+[K])\{\varphi\}_i} \tag{37}$$

Developing the denominator of the previous equation,

$$\bar{b}_{ij,o}=i\omega_i^2\frac{\{\varphi\}_i^T[\bar{g}_j]\{\varphi\}_i}{\omega_i^2\{\varphi\}_i^T[M]\{\varphi\}_i+\{\varphi\}_i^T[K]\{\varphi\}_i} \tag{38}$$

If normalized modes are used with respect to the mass matrix, the following expressions apply:

$$\left.\begin{array}{c}\{\varphi\}_i^T[M]\{\varphi\}_i=1\\ \{\varphi\}_i^T[K]\{\varphi\}_i=\omega_i^2\end{array}\right\} \tag{39}$$

Substituting in Eq. (38),

$$\bar{b}_{ij,o}=i\omega_i^2\frac{\{\varphi\}_i^T[\bar{g}_j]\{\varphi\}_i}{\omega_i^2+\omega_i^2} \tag{40}$$

and, simplifying,

$$\bar{b}_{ij,o}=i\tfrac{1}{2}\{\varphi\}_i^T[\bar{g}_j]\{\varphi\}_i \tag{41}$$

To understand the expression of the effectiveness index $\bar{b}_{ij,o}$, it is convenient to realize the meaning of the real and imaginary parts of a complex eigenvalue in a damped dynamic system. Let $\Omega_i$ be expressed as

$$\Omega_i=\mathrm{Re}(\Omega_i)+i\mathrm{Im}(\Omega_i) \tag{42}$$

where $\mathrm{Re}(\Omega_i)$ and $\mathrm{Im}(\Omega_i)$ are the real and imaginary parts of a complex eigenvalue. In accordance with Eq. (23),

$$s=i(\mathrm{Re}(\Omega_i)+i\mathrm{Im}(\Omega_i)) \tag{43}$$

that is,

$$s=-\mathrm{Im}(\Omega_i)+i\mathrm{Re}(\Omega_i) \tag{44}$$

Returning to Eq. (23),

$$\{\delta(t)\}=\{\psi\}e^{-\mathrm{Im}(\Omega_i)t}e^{i\mathrm{Re}(\Omega_i)t} \tag{45}$$

The real part of $\Omega_i$ is the damped vibration frequency, and the imaginary part corresponds to the exponent of the logarithmic decrement of the vibration amplitude. Therefore, when the $\Omega_i$ complex eigenvalue is analyzed, the most interesting part to define the effectiveness indices is the imaginary part because the aim is to study the possibility of reducing the vibration amplitude and, more precisely, the sensitivity of this amplitude to the allocation of dampers in different locations. In the case of Eq. (41), the expression of the derivative of $\Omega_i$ in the initial situation without dampers only has an imaginary part. For simplicity, the effectiveness index is redefined as

$$b_{ij,o}=\{\varphi\}_i^T[\bar{g}_j]\{\varphi\}_i \tag{46}$$

where

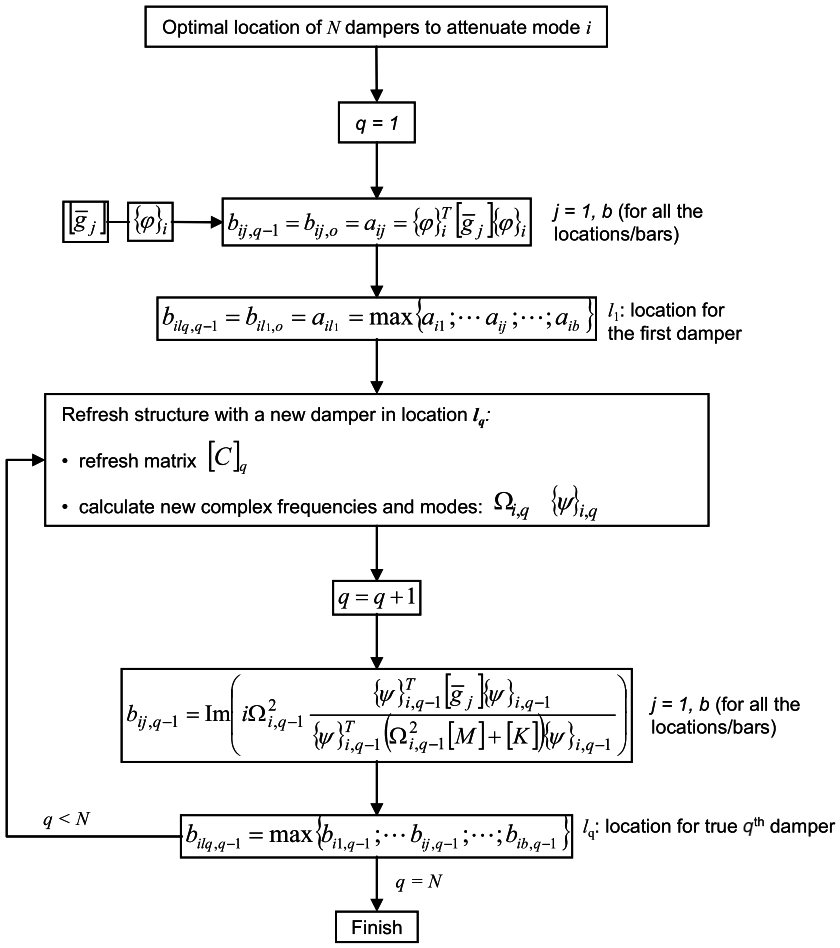


**Fig. 10 Optimal locations of $N$ dampers to attenuate the mode $i$ via complex indices.**

$$\bar{b}_{ij,o} = \frac{\partial \Omega_i}{\partial c_j} = i\frac{1}{2} b_{ij,o} \tag{47}$$

The first conclusion of this development is that, according to Eq. (10), the effectiveness index $b_{ij,o}$ in the initial situation without any damper in the VGT is identical to the real effectiveness index defined in Sec II:

$$b_{ij,o} = a_{ij} \tag{48}$$

It is shown that the real eigensensitivity with respect to the stiffness of the bars and the complex eigensensitivity in relation to the damping coefficients of the possible dampers parallel to the previous bars are identical when a nondamped structure is used as the starting point.

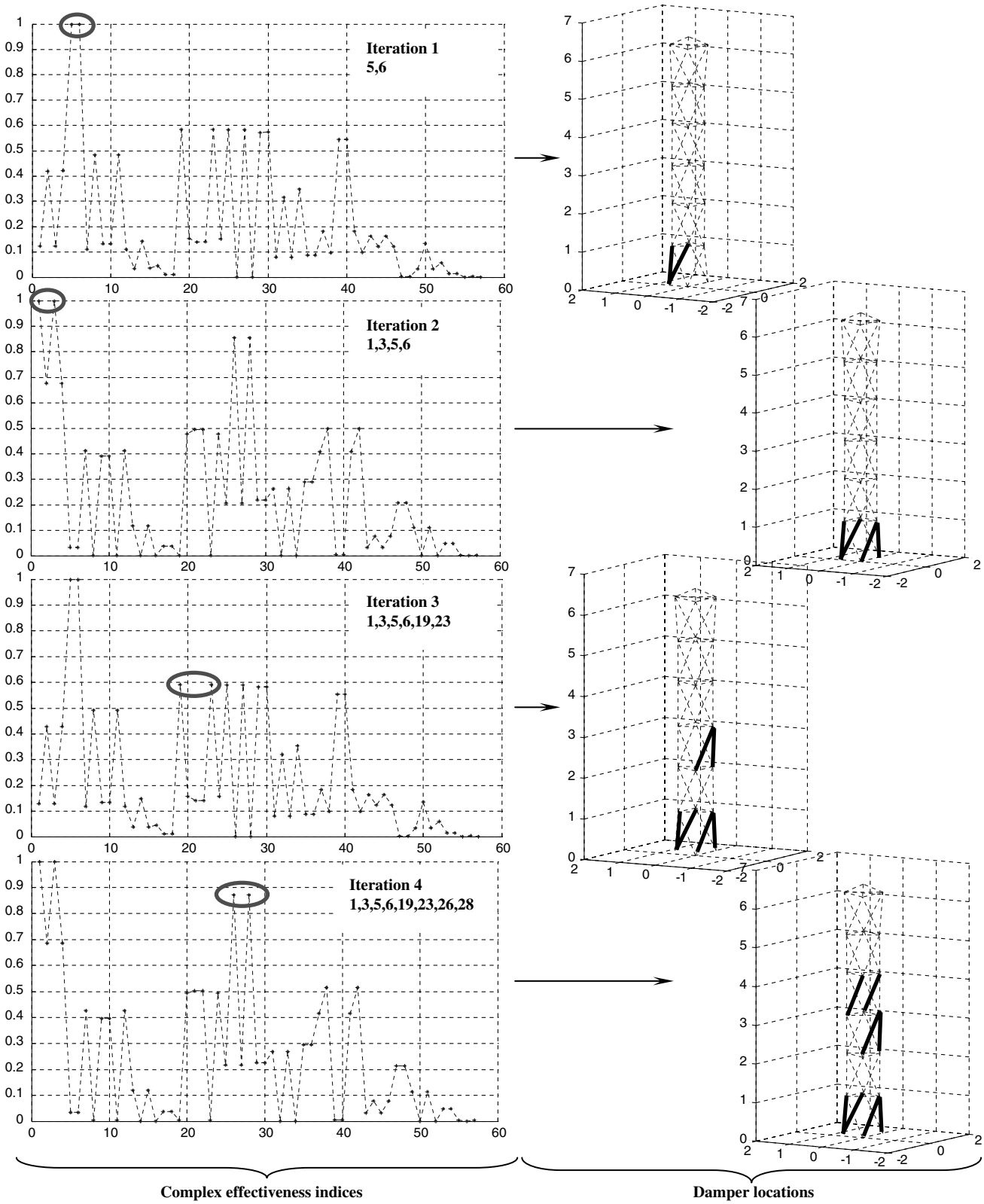


**Fig. 11 Successive location of dampers to attenuate the fourth vibration mode.**

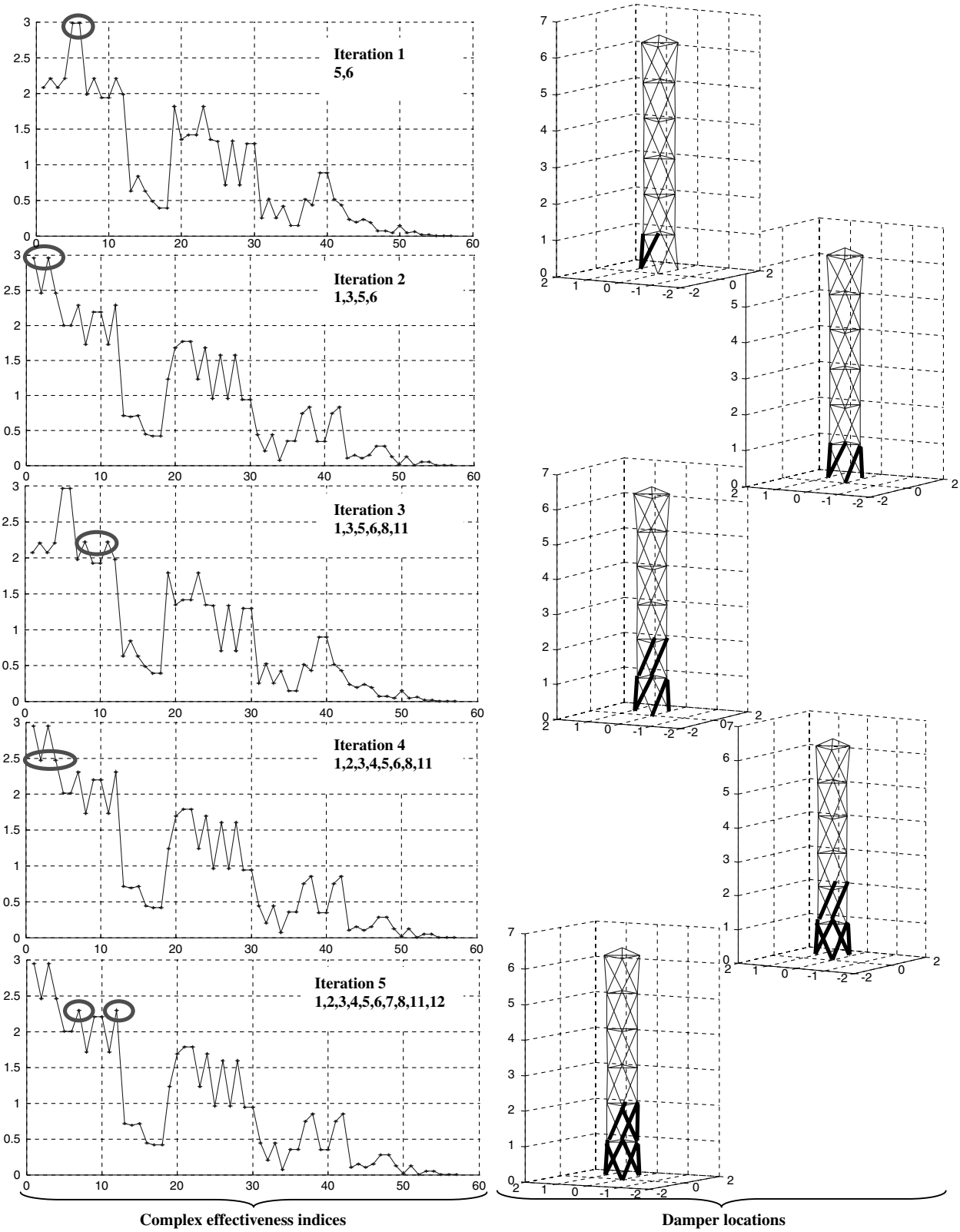


**Fig. 12 Successive location of damping elements for the four lowest vibration modes.**

Until now, the development of new effectiveness indices has not provided any additional information with respect to those developed in Sec. II, except for the ratification achieved via a different analysis. However, this new development allows the consideration of the perturbation effect caused by the dampers over vibration modes, without having to resort to a simplified analysis neglecting the difference between the damped and real modes.

This proposed general methodology involves the allocation of dampers one by one, or group by group, recalculating the effectiveness indices when a new damper or group of dampers is located. In this way, when dampers are added one by one, the first damper will be placed where $b_{ij,o} = a_{ij}$ is maximum, that is, where the real effectiveness index of the original nondamped structure is maximum. It has to be taken into account that, with this approach, the

full structure has been considered; therefore, a global optimum location is achieved. Then, the $b_{ij,1}$ effectiveness index will be calculated for the structure with one damper as calculated in the previous step to locate the second one. For the third damper, the $b_{ij,2}$ effectiveness index will be calculated for the structure that already has two dampers, and so on. For $N$ dampers to be included, $N$ iterations will have to be solved.

Rewriting Eq. (35) in a general form for the $q$th iteration,

$$\bar{b}_{ij,q-1} = i\Omega_{i,q-1}^2 \frac{\{\psi\}_{i,q-1}^T[\bar{g}_j]\{\psi\}_{i,q-1}}{\{\psi\}_{i,q-1}^T(\Omega_{i,q-1}^2[M]+[K])\{\psi\}_{i,q-1}} \tag{49}$$

where $\bar{b}_{ij,q-1}$ is a complex number. The imaginary part is the most interesting one, as shown in Eq. (45). Actually, what is being considered is the modal damping derivative with respect to the damping coefficients. Thus, the following expression can be used as the effectiveness index of location $j$ for vibration complex mode $i$:

$$b_{ij,q-1} = \mathrm{Im}\left(i\Omega_{i,q-1}^2 \frac{\{\psi\}_{i,q-1}^T[\bar{g}_j]\{\psi\}_{i,q-1}}{\{\psi\}_{i,q-1}^T(\Omega_{i,q-1}^2[M]+[K])\{\psi\}_{i,q-1}}\right) \tag{50}$$

The flowchart in Fig. 10 shows the methodology to search for the optimal locations of $N$ dampers to attenuate the complex vibration mode $i$. When the structure was initially damped, the first $b_{ij,0}$ should be avoided and the process should start with $b_{ij,1}$.

## V. Examples of Damper Positioning Using Complex Eigensensitivity

The VGT of Fig. 2 is considered in this section, as in the examples developed in Sec. III. In the following paragraphs, a set of examples are shown using the derivatives of the complex eigenvalues as effectiveness indices.

### A. Example 1

It is supposed that vibrations exciting the fourth mode are to be attenuated. Using complex effectiveness indices, discrete dampers with a damping coefficient of $1.0 \times 10^4$ N · s/m are to be placed along the structure. Because of physical limitations, only one damper is to be arranged in each location. In Fig. 11, four iterations are shown and, in each iteration, a set of two dampers is located.

In the first iteration, locations 5 and 6 correspond to maximum effectiveness index values; therefore, two dampers are located there.

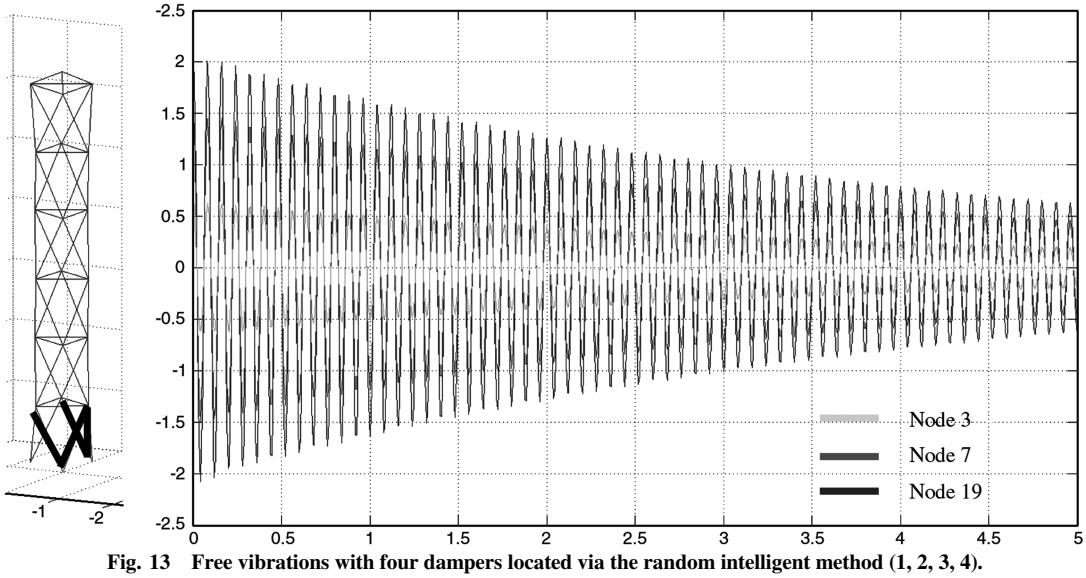


**Fig. 13 Free vibrations with four dampers located via the random intelligent method (1, 2, 3, 4).**

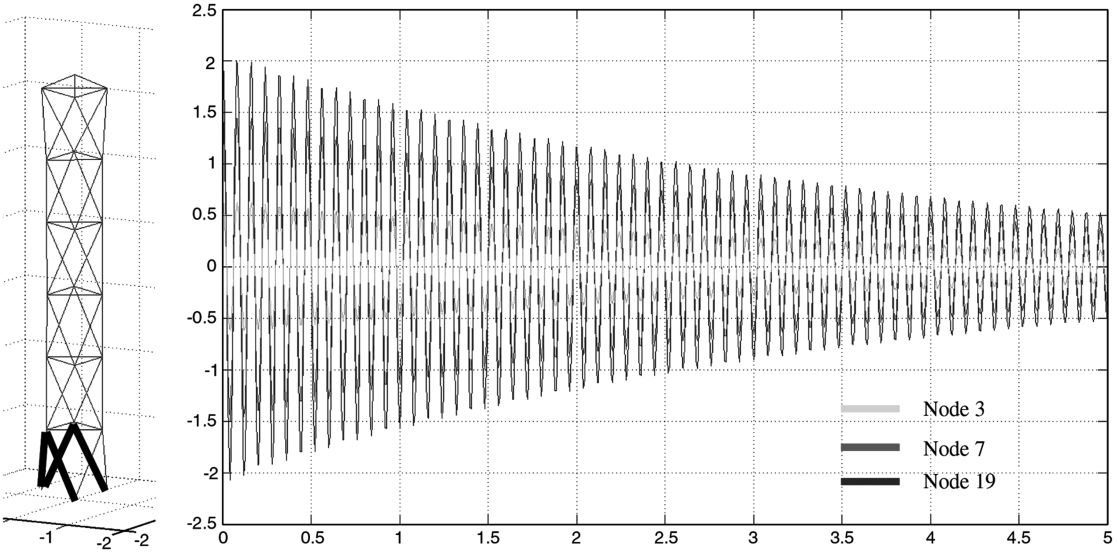


**Fig. 14 Free vibrations with four dampers located via real eigensensitivity (2, 4, 5, 6).**

In the second iteration, locations 1 and 3 show the highest eigensensitivity once the previous dampers are included in the VGT. One can state that the system is now "balanced" in terms of damper placement.

Before the third iteration, dampers in locations 1, 3, 5, and 6 have been placed; afterward, when complex eigenvalue derivatives are recalculated, locations 5 and 6 correspond again to the highest values. As stated at the beginning of the example, only one damper is allowed in each location; thus, locations 19 and 23 have been chosen because they are the next locations where effectiveness values are the highest. In the fourth and last iteration, the new eigensensitivities are calculated with the VGT with dampers in locations 1, 3, 5, 6, 19, and 23. The locations with higher eigensensitivity are again numbers 1 and 3. As these locations are already occupied by dampers, the next possible locations are numbers 26 and 28.

### B. Example 2

The same example is analyzed, but now the attenuation of the four lowest modes is considered instead of only the fourth mode. In this case, discrete dampers are also placed in sets of two with a damping constant $c$ with a value of $1.0 \times 10^4$ N · s/m. Successive iterations are shown in Fig. 12.

## VI. Comparison of Damper Positioning with Real Eigensensitivity, Complex Eigensensitivity, and "Random Intelligent" Damper Positioning

In this last section, a comparative analysis of different damper positioning methods is performed. Two of them are the methods described in this paper: the real eigensensitivity method and complex eigensensitivity method. The third one is a random intelligent method, that is, a method in which the location of the dampers is chosen via engineering reasoning, attending to the shape of modes to be attenuated. It also would be valuable to take into account a comparison with a full search method but, from the computational point of view, it is not a viable option for complex structures, and the results obtained with a simpler structure would not be representative. Once the fourth option has been ruled out for the three first cases, the horizontal displacements of nodes 7, 13, and 19, placed at different heights along the structure, will be measured for a certain length of time. The comparison is performed for the following cases:

1) *Free vibrations*: The starting point is the static deformation caused from the application of a horizontal force of 100 kN to the upper node of the structure in the direction given by nodes 1–2 (from 1 toward 2). This direction has been chosen to excite bending modes. Then, the structure is allowed to vibrate freely.

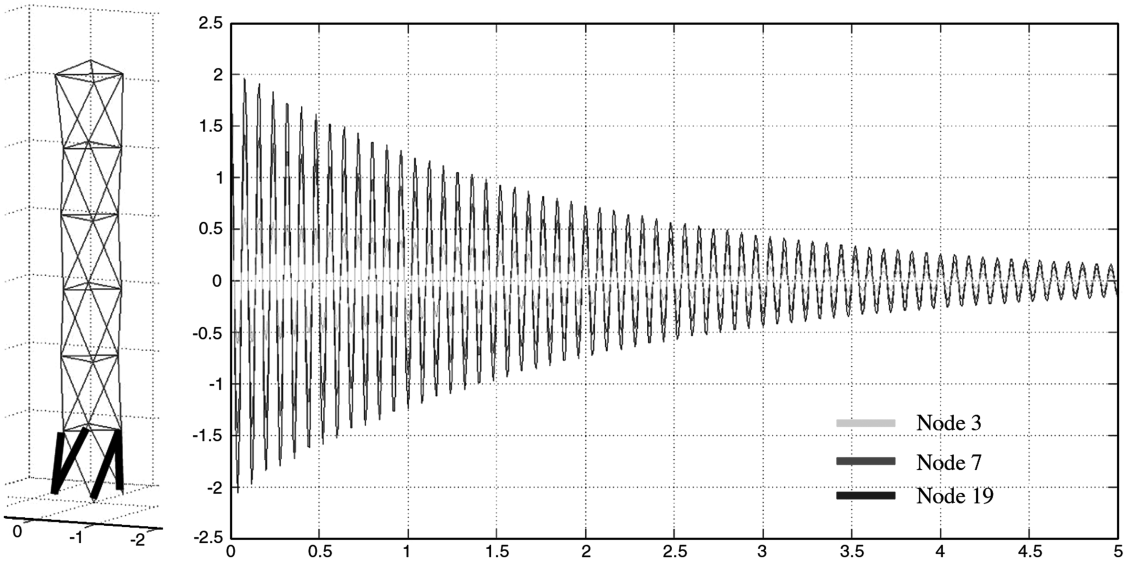


**Fig. 15 Free vibrations with four dampers located via complex eigensensitivity (1, 3, 5, 6).**

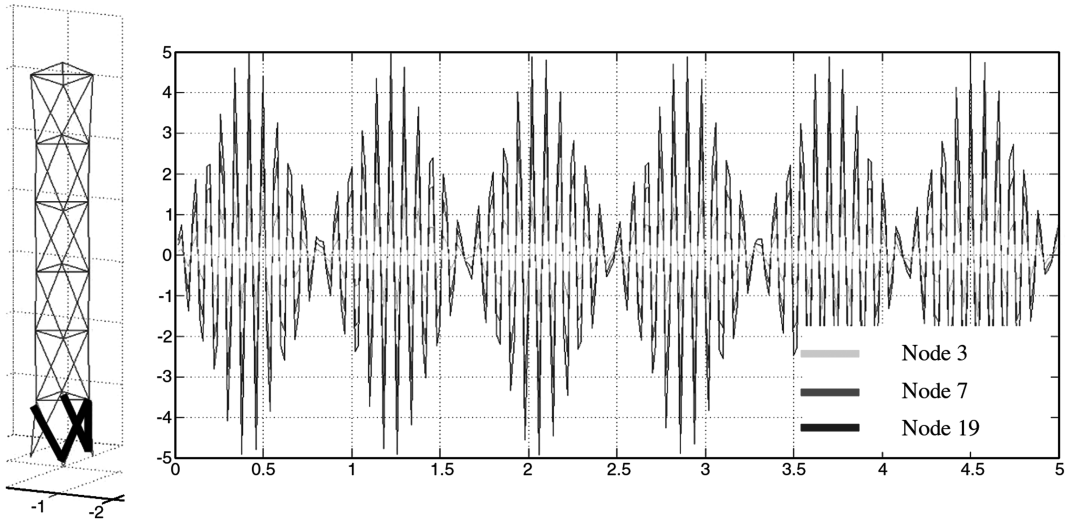


**Fig. 16 Forced vibrations with four dampers located via "random intuitive" method (1, 2, 3, 4).**

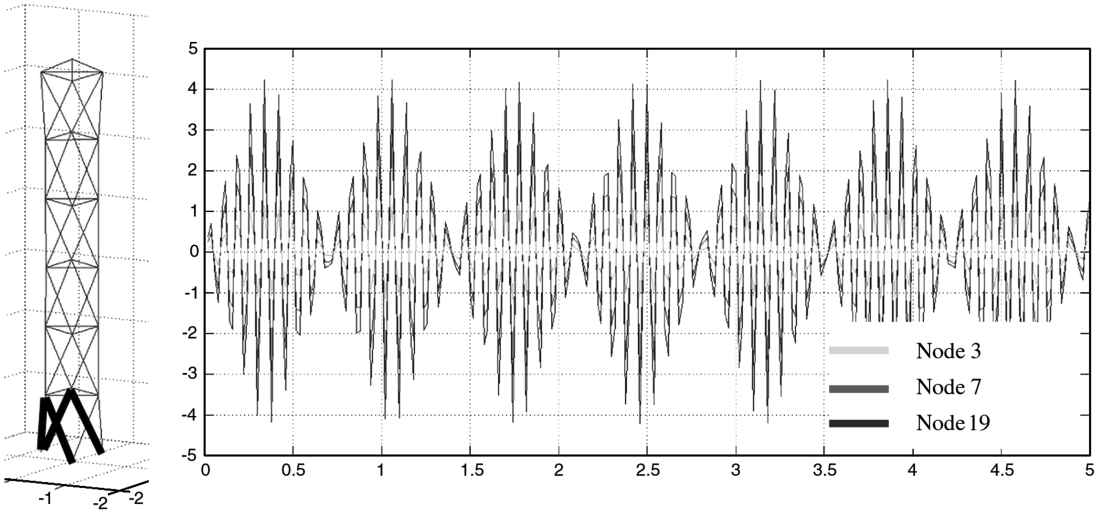


**Fig. 17 Forced vibrations with four dampers located via real eigensensitivity (2, 4, 5, 6).**

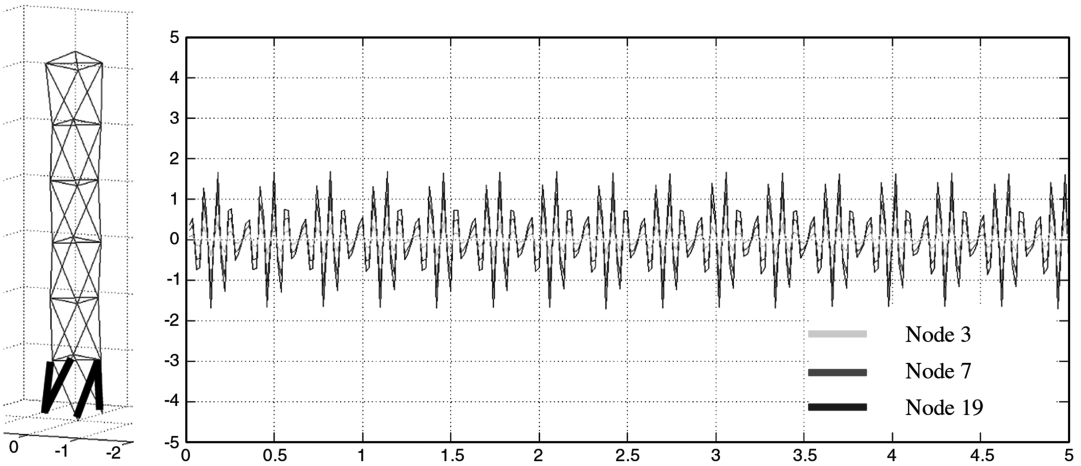


**Fig. 18 Forced vibrations with four dampers located via complex eigensensitivity (1, 3, 5, 6).**

2) *Forced vibrations*: The system is excited with a harmonic force at the upper node and in the same direction as in case 1. The amplitude is 50E03 N, and it has two harmonic terms; one has an excitation frequency of 12.5 Hz and the other 60 Hz, that is, $F(t) = 50\text{E}03[\sin(2\pi 12.5 \times t) + \sin(2\pi 60 \times t)]$. These harmonic terms should excite more or less the lowest four natural frequencies, as their values for the nondamped structure are $f1 = 12.523$ Hz, $f2 = 12.524$ Hz, $f3 = 56.96$ Hz, $f4 = 67.31$ Hz.

The value of the damping coefficients is $1.0 \times 10^4$ N $\cdot$ s/m. The distributions of dampers to be chosen must take into account the four lowest modes. In Figs. 13–18, the effectiveness of each method can be appreciated. In both types of vibrations, free and forced, a sensible difference can be observed among the results. The methods developed here have a better performance than an intuitive election of the damper location. In addition, one can observe that, between the two methods developed here, the complex eigensensitivity method is more effective than the real eigensensitivity method.

## VII. Conclusions

In this paper, two procedures have been developed to calculate the optimal damper distributions in variable geometry trusses. These procedures are based on eigensensitivity, that is, the calculation of the derivatives of natural eigenfrequencies and eigenmodes with respect to dynamic parameters of the VGT. The derivation with respect to the stiffness parameters leads to the first of these methods, called the real eigensensitivity method; the derivation performed with respect to the damping parameters gives rise to the second one, called the complex eigensensitivity method. In the first method, the derivatives of frequencies are performed for the nondamped structure; therefore, all the dampers are located in one go. The second method requires the calculation of the derivatives of the complex eigenvalues of the structure once damped. Thus, progressive damping placement is done iteratively until a maximum number of dampers are placed; to incorporate a new damper (or damper subset), the eigensensitivity for the damped structure is assessed with the damper distribution of the last iteration. Results have been compared in terms of the dynamic response, and the effectiveness of the two proposed methods has been proven. The complex eigensensitivity method has been shown to be particularly effective in the examples presented in this paper. However, there is challenging work to be done in the future to refine the method of optimum damper location; the authors are now dealing with the hybridization of this methodology with genetic algorithms.

## Acknowledgments

This study is a part of a series of studies of the Department of Mechanical Engineering of the University of the Basque Country dealing with several kinematic and dynamic aspects of highly redundant multibody systems. The work is supported by the Spanish Ministry of Education and Science through project DPI2001-0074.

## References

[1] Keane, A. J., and Bright, A. P., "Passive Vibration Control via Unusual Geometries: Experiments on Model Aerospace Structures," *Journal of*

*Sound and Vibration*, Vol. 185, No. 3, 1995, pp. 441–453. doi:10.1006/jsvi.1995.0391

[2] Keane, A. J., "Passive Vibration Control via Unusual Geometries: The Application of Genetic Algorithm Optimization to Structural Design," *Journal of Sound and Vibration*, Vol. 190, No. 4, 1996, pp. 713–719. doi:10.1006/jsvi.1996.0086

[3] Nair, P. B., and Keane, A. J., "Passive Vibration Suppression of Flexible Space Structures via Optimal Geometric Design," *AIAA Journal*, Vol. 39, No. 7, 2001, pp. 1338–1346. doi:10.2514/2.1452

[4] Skelton, R. E., and DeLorenzo, M. L., "Selection of Noisy Actuators and Sensors in Linear Stochastic Systems," *Large Scale Systems, Theory and Applications*, Vol. 4, International Federation of Automatic Control, Laxenburg, Austria, 1983, pp. 109–136.

[5] Haftka, R. T., and Adelman, H. M., "Selection of Actuator Locations for Static Shape Control of Large Space Structures by Heuristic Integer Programming," *Computers and Structures*, Vol. 20, 1985, pp. 575–582. doi:10.1016/0045-7949(85)90105-1

[6] Burdisso, R. A., and Haftka, R. T., "Statistical Analysis of Static Shape Control in Space Structures," *AIAA Journal*, Vol. 28, No. 8, 1990, pp. 1504–1508. doi:10.2514/3.25245

[7] Maghami, P. G., and Joshi, S. M., "Sensor-Actuator Placement for Flexible Structures with Actuator Dynamics," *Proceedings AIAA Guidance, Navigation and Control Conference*, AIAA, Washington, D.C., Aug. 1991, pp. 12–14.

[8] Preumont, A., Dufour, J. P., and Sparavier, M., "Active Damping of a Truss Structure Using Piezoelectric Actuators. The Dynamics of Flexible Structures in Space," *Proceedings of the 1st International Conference on Dynamics of Flexible Structures in Space*, Springer–Verlag, Berlin/New York/Heidelberg, May 1990, pp. 369–382.

[9] Lammering, R., Jia, J., and Rogers, C. A., "Optimal Placement of Piezoelectric Actuators in Adaptive Truss Structures," *Journal of Sound and Vibration*, Vol. 171, No. 1, 1994, pp. 67–85. doi:10.1006/jsvi.1994.1104

[10] Ponslet, E., Haftka, R. T., Halluer, W. L., and Cudney, H. H., "Desensitizing Structural Control Design," *Journal of Guidance, Control, and Dynamics*, Vol. 17, 1994. pp. 175–180. doi:10.2514/3.21175

[11] Padula, S. L., and Sandridge, C. A., "Passive/active strut placement by integer programming," *Topology Design of Structures*, edited by M. P. Bensoe, and C. A. Mota Soares, Kluwer Academic, , Norwell, MA, 1993, pp. 145–156.

[12] Metropolis, N., and Rosenbluth, A. W., Rosenbluth, M. N., Teller, A. H., and Teller, E., "Equation of State Calculations by Fast Computing Machines," *Journal Chemical Physics*, Vol. 21, No. 6, 1953, pp. 1087–1092. doi:10.1063/1.1699114

[13] Chen, G. S., Lurie, B. J., and Wada, B. K., "Experimental Studies of Adaptive Structures for Precision Performance," AIAA Paper 89-1327-CP, 1989.

[14] Chen, G. S., Bruno, R. J., and Salama, M., "Optimal Placement of Active/Passive Members in Structures Using Simulated Annealing," *AIAA Journal*, Vol. 29, No. 8, 1991, pp. 1327–1334. doi:10.2514/3.10739

[15] Holland, J. H., *Adaptation in Natural and Artificial Systems*, Univ. of Michigan Press, Ann Arbor, MI, 1975.

[16] Rao, S. S., Pan, T. S., and Venkayya, V. B., "Optimal Placement of Actuators in Actively Controlled Structures Using Genetic Algorithms," *AIAA Journal*, Vol. 29, No. 6, 1991, pp. 942–943. doi:10.2514/3.10683

[17] Onoda, J., and Hanawa, Y., "Actuator Placement Optimization by Genetic and Improved Simulated Annealing Algorithms," *AIAA Journal*, Vol. 31, No. 6, 1993, pp. 1167–1169. doi:10.2514/3.49057

[18] Dhingra, A. K., and Lee, B. H., "Optimal Placement of Actuators in Actively Controlled Structures," *Engineering optimization*, Vol. 23, 1994, pp. 99–118. doi:10.1080/03052159408941347

[19] Furuya, H., and Haftka, R. T., "Placing Actuators on Space Structures by Genetic Algorithms and Effectiveness Indices," *Structural optimization*, Vol. 9, 1995, pp. 69–75. doi:10.1007/BF01758822

[20] Abdullah, M., Richardson, A., and Hanif, J., "Placement of Sensors/Actuators on Civil Structures Using Genetic Algorithms," *Earthquake Engineering and Structural Dynamics*, Vol. 30, 2001, pp. 1167–1184. doi:10.1002/eqe.57

[21] Singh, M. P., and Moreschi, L. M., "Optimal Placement of Dampers for Passive Response Control," *Earthquake Engineering and Structural Dynamics*, Vol. 31, 2002, pp. 955–976. doi:10.1002/eqe.132

[22] Wongprasert, N., and Symans, M. D., "Optimal Distribution of Fluid Dampers for Control of the Wind Benchmark Problem," *Proceedings of 14th ASCE Engineering Mechanics Conference*, May 2000, http://www.ce.utexas.edu/em2000/papers/NatWong.pdf.

[23] Wongprasert, N., and Symans, M. D., "Application of a Genetic Algorithm for Optimal Damper Distribution Within the Nonlinear Seismic Benchmark Building," *Journal of Engineering Mechanics*, Vol. 130, No. 4, 2004, pp. 401–406. doi:10.1061/(ASCE)0733-9399(2004)130:4(401)

[24] Cheng, F. Y., Jiang, H., and Zhang, X., "Optimal Placement of Dampers and Actuators Based on Stochastic Approach," *Earthquake Engineering and Engineering Vibration*, Vol. 1, No. 2, 2002, pp. 237–249. doi:10.1007/s11803-002-0069-y

[25] Yan, Y. J., and Yam, L. H., "Optimal Design of Number and Locations of Actuators in Active Vibration Control of a Space Truss," *Smart Materials and Structures*, Vol. 11, 2002, pp. 496–503. doi:10.1088/0964-1726/11/4/303

[26] Fox, R. L., and Kapoor, M. P., "Rates of Change of Eigenvalues and Eigenvectors," *AIAA Journal*, Vol. 6, No. 12, 1968, pp. 2426–2429. doi:10.2514/3.5008

[27] Adhikari, S., "Rates of Change of Eigenvalues and Eigenvectors in Damped Dynamic System," *AIAA Journal*, Vol. 37, No. 11, 1999, pp. 1452–1457. doi:10.2514/2.622

[28] Avilés, R., Ajuria, M. B. G., Gómez-Garay, V., and Navalpotro, S., "Comparison Among Nonlinear Optimization Methods for the Static Equilibrium Analysis of Multibody Systems with Rigid and Elastic Elements," *Mechanism and Machine Theory*, Vol. 35, No. 8, 2000, pp. 1151–1168. doi:10.1016/S0094-114X(99)00053-1

[29] Avilés, R., Vallejo, J., Ajuria, G., and Agirrebeitia, J., "Second-Order Methods for the Optimum Synthesis of Multibody Systems," *Structural and Multidisciplinary Optimization*, Vol. 19, No. 3, 2000, pp. 192–203. doi:10.1007/s001580050102

[30] Gao, W., "Stochastically Optimal Active Control of a Smart Truss Structure Under Stationary Random Excitation," *Journal of Sound and Vibration*, Vol. 290, 2006, pp. 1256–1268. doi:10.1016/j.jsv.2005.05.019

[31] Bilbao, A., Avilés, R., Agirrebeitia, J., and Ajuria, G., "Proportional Damping Approximation for Structures with Added Viscoelastic Dampers," *Finite Elements in Analysis and Design*, Vol. 42, No. 6, 2006, pp. 492–502. doi:10.1016/j.finel.2005.10.001

A. Messac
*Associate Editor*